Deep learning based dental implant failure prediction from periapical and panoramic films

Chunan Zhang[1#], Linfeng Fan[2#], Shisheng Zhang[3], Jun Zhao[4], Yingxin Gu[1]

[1]Department of Implant Dentistry, Shanghai Ninth People's Hospital, College of Stomatology, Shanghai Jiao Tong University School of Medicine, Shanghai Key Laboratory of Stomatology, National Center for Stomatology, National Clinical Research Center for Oral Diseases, Shanghai, China; [2]Department of Radiology, Shanghai Ninth's People Hospital, Shanghai Jiao Tong University School of Medicine, Shanghai, China; [3]Intanx Life (Shanghai) Co., Ltd., Shanghai, China; [4]School of Biomedical Engineering, Shanghai Jiaotong University, Shanghai, China

Contributions: (I) Conception and design: C Zhang, J Zhao; (II) Administrative support: Y Gu; (III) Provision of study materials and patients: C Zhang, L Fan; (IV) Collection and assembly of data: C Zhang, L Fan; (V) Data analysis and interpretation: L Fan, S Zhang; (VI) Manuscript writing: All authors; (VII) Final approval of manuscript: All authors.

[#]These authors have contributed equally to this work.

Correspondence to: Jun Zhao. School of Biomedical Engineering, Shanghai Jiao Tong University, No. 800, Dong Chuan Road, Shanghai 200030, China. Email: junzhao@sjtu.edu.cn; Yingxin Gu. Department of Implant Dentistry, Shanghai Ninth People's Hospital, Shanghai Jiao Tong University School of Medicine, 639 Zhizaoju Road, Shanghai 200011, China. Email: yingxingu@163.com.

Background: Dental implant failure is a critical condition that can seriously compromise therapeutic efficacy. Insufficient bone volume, unfavorable bone quality, periodontal bone loss, and systemic conditions, including osteopenia/osteoporosis and diabetes mellitus, have been associated with implant failure. Early indicators of potential implant failure could help mitigate the risk of severe complications. This study aimed to develop an effective implant outcome prediction model using dental periapical and panoramic films.

Methods: A total of 248 patients (89 with failed implants and 159 with successful implants) were examined. A total of 529 periapical images and 551 panoramic images were collected from the patients for a deep learning-based model. Based on radiographic peri-implant alveolar bone pattern, implant outcome was divided into three categories: implant failure with marginal bone loss, implant failure without marginal bone loss, and implant success. We extracted features using a deep convolutional neural network (CNN) and built a hybrid model to combine periapical and panoramic images. A comparison among three categories of receiver operating characteristic (ROC) curves was performed. The diagnostic accuracy, precision, recall and F1-score of the dataset were assessed.

Results: Our model achieved an AUC (area under the ROC curve) of 0.972 for failure with marginal bone loss, 0.947 for failure without marginal bone loss and 0.975 for success. In all conditions, for periapical images alone, the diagnostic accuracy was 78.6%; the precision was 0.84, recall was 0.73, and F1-score was 0.75. For panoramic images alone, the diagnostic accuracy was 78.7%; the precision was 0.87, recall was 0.63, and F1-score was 0.66. Both periapical and panoramic images were used in our novel method, and the prediction accuracy was 87%. The precision was 0.85, recall was 0.88, and F1-score was 0.85.

Conclusions: The deep learning model used features from periapical and panoramic images to effectively predict the occurrence of implant failure and might facilitate early clinical intervention for potential dental implant failures.

Keywords: Dental implant failure; deep learning; periapical film; panoramic radiography; convolutional neural network (CNN)

Introduction

Recently, dental implant treatment has become more common, with high survival rates and patient satisfaction. Although failure rates are reportedly low (around 5%), an estimated 20,000 of the almost 400,000 new implants in China fail each year (1). This failure number is frustrating for both patients and doctors. There are many risk factors for implant outcomes such as inferior anatomical structures and inadequate spacing (2), implant location with different alveolar bone characteristics (3), infection (4), smoking (5), surgery procedure and planning (6), and medical compromised condition such as osteopenia/osteoporosis and diabetes mellitus (7,8). Analytical and objective methods are therefore urgently needed to predict implant failure.

In fact, radiographic information has been associated with several risk factors that may affect implant outcome, including insufficient bone volume, unfavorable bone quality, as well as periodontal bone loss (9). Nicolielo *et al.* suggested that mandibular preoperative trabecular bone structure from cone beam computed tomography (CBCT) could provide important indications for early implant failure risk (10). This is consistent with clinical observations that implant failure is seen more often in dense bone, which usually presents low blood flow. Moreover, studies have used radiographic images to establish implant prediction models. Huang et al. used preoperative CBCT to extract image features to create a deep learning model that predicted implant loss (11). Although CBCT has its obvious advantage of 3-dimensional view, this method generally involves a higher radiation dose compared to conventional 2-dimensional panoramic or periapical films. In fact, for non-complex cases, scrutinized clinical examination combined with panoramic films were enough for preoperative evaluation. Moreover, in most conditions, CBCT is used for presurgical diagnosis and preoperative planning. However, the postoperative application of CBCT is restricted by titanium artifact and excessive dose compared to periapical films, which could give information in osseointegration, marginal bone loss, or implant failure.

From clinical observation, two types of implant failure manifest in periapical film. The first one is described as typical crater-like marginal bone loss around implants, in which peri-implantitis has a high prevalence (12,13). Generally, inflammation is the main cause for peri-implantitis, which could lead to implant failure (14). In this case, patients need to undergo several surgical and non-surgical treatments to restore and regenerate lost bone, and then undergo re-implant operation, which is laborious and costly. Therefore, the early prediction of marginal bone loss would allow dentists to identify possible peri-implantitis and intervene while symptoms are mild.

The other typical implant failure occurs owing to the development of fibrous tissue between implant and surrounding bone, without obvious marginal bone loss. Unlike successful osseointegration with intact bone-implant contact, a characteristic feature is the presence of around 0.5 mm peri-implant radiolucency (15). However, due to 3-dimensional bone structure superimposition in periapical film, identification of osseointegration can be difficult. Moreover, unlike failure with marginal bone loss, the histopathological mechanism of this type of failure has not yet been fully understood. From clinical experience, there are many possible reasons for failure without marginal bone loss such as unfavorable bone quality, periodontitis, surgical procedure, medical compromised situation such as diabetes and osteopenia/osteoporosis, which might exert harmful effects on bone metabolism. Moreover, the osseointegration status in periapical radiography might be ambiguous, leading to variable clinical interpretation (16). Under this condition, loading before adequate osseointegration may lead to future failure.

Up to now, there is no valid method to evaluate alveolar bone status around implants in radiographic images objectively (17). AI algorithms can provide a powerful diagnostic tool to capture characteristic patterns using radiographic images in dentistry (18). Currently, it is suggested that alveolar radiographic characteristics can predict implant failure (10), and some methods have shown efficacy in extracting characteristics from radiographs (19-21). One study has used CBCT images with algorithms for model training to analyze risk factors for dental implant outcome (11). However, there have been no studies using panoramic and periapical films to predict implant fate. Moreover, research on the use of hybrid images with panoramic and periapical films is limited. Our study thus aimed to develop
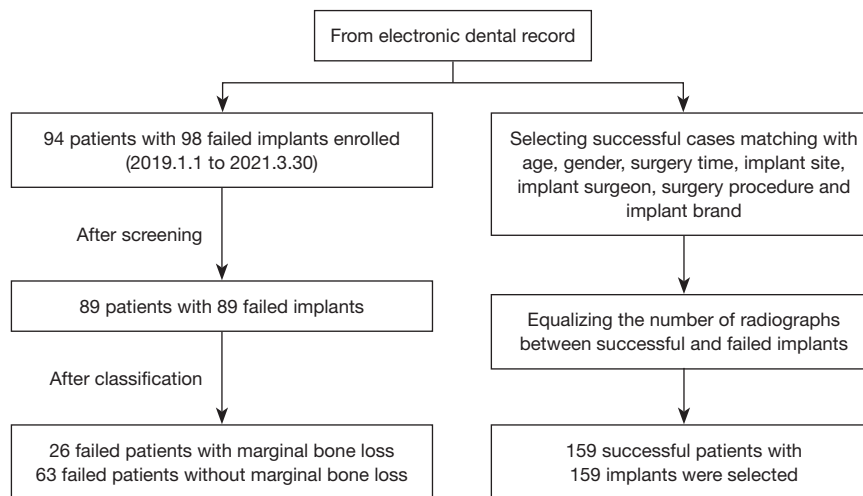
Figure 1 Flow chart for case enrolling and selecting.

a deep learning-based method to predict the occurrence of implant failure with panoramic and periapical images using convolutional neural networks (CNNs) to extract features from preprocessed images. Under this model, the output would indicate whether the implant will be successful, fail with marginal bone loss, or fail without marginal bone loss. We present this article following in accordance with the TRIPOD reporting checklist (available at https://qims.amegroups.com/article/view/10.21037/qims-22-457/rc).

Methods

Ethical statement

The study was conducted in accordance with the Declaration of Helsinki (as revised in 2013). The study was approved by Medical Ethics Committee of the Shanghai Ninth People's Hospital (No. SH0H-2021-T469-1: the registration number of ethics board). As only deidentified radiographic information was obtained in this retrospective study, informed consent from patients was waived.

Patient information

This study was conducted at the Department of Implant Dentistry from Shanghai Ninth People's Hospital. We retrospectively screened failed implants from January 2019 to March 2021. The inclusion and exclusion criteria are detailed as follows:

(I) Inclusion criteria
    (i) Implant failure between 2019.1.1–2021.3.30

from Electronic Dental Record (EDR);
    (ii) One patient should at least have two films including a pre-op panoramic film and a post-op periapical film before second-stage surgery or impression taking (time between the exams were generally 2.5–9 months).

(II) Exclusion criteria
    (i) Incomplete radiographic information;
    (ii) Radiographic films with poor quality such as movement artifacts;
    (iii) Implants with immediate implantation and loading;
    (iv) Multiple implant placements at one area.

The enrolling and selecting process is shown in *Figure 1*.

Data collection

Deidentified periapical radiographic image datasets and panoramic radiographic image datasets obtained with Heliodent Plus and Orthophos XG5 (Sirona, Bensheim, Germany) were collected, respectively. For periapical films, bisector technique was adopted. Owing to retrospective nature of this study, no positioner was used. The exposure settings were 70 kV, 7 mA for 0.08 s. After exposure, films were digitized with a DIGORA Optime machine (Soredex, Milwaukee, WI, USA). For panoramic films, a standard chin rest and head stabilizer were used. The exposure settings were 80 kV, 8 mA for 7.2 s. Images were digital and then uploaded for doctors to check online. All images were validated and downloaded from Picture Archiving

Figure 2 Illustration of input images (left: success, middle: failure with marginal bone loss, right: failure without marginal bone loss).

Table 1 Detailed information of the groups of patients

Group	Sex (number)		Age (years), (mean ± SD)	Time (months), median (interquartile range)	Upper jaw (number)		Lower jaw (number)	
	Male	Female			Anterior	Posterior	Anterior	Posterior
Failure with marginal bone loss	14	12	52.54±15.49	14 (23.25)	4	7	3	12
Failure without marginal bone loss	37	26	51.62±16.14	8 (12.0)	13	22	7	21
Success	91	68	51.67±16.02	15 (17.5)	29	54	16	60

Communication System (PACS) by one radiologist (LFF, a certified radiologist).

Sample calculation and collection

Based on a previous study (9), the adopted odds ratio value was 4.96 and P0 was 0.1. Combined with 0.05 alpha and 0.9 power, the required sample size was 135 (45 failure plus 90 success; N2/N1=2), which was calculated through PASS software (version 15.0.3, NCSS, Kaysville, UT, USA). Clinically, as patients with failed implants tended to have more radiographs before and after re-implant surgery, thus we set the number in N2 (success) twice as in N1 (fail) to equalize the number of final radiographs between two groups. However, based on deep learning requirement of more radiographs, we wanted an even larger sample size. Thus, we collected all implant failure cases from January, 1, 2019, and March 30, 2021. After screening, the final number we collected was 89. Based on acquired information with patients' age, gender, surgery time, implant site, implant surgeon, surgery procedure and implant brand, we manually selected 159 patients with successful implants. All enrolled

cases received implant placement with implant outcome recorded in EDR. Furthermore, to better characterize implant failure, we divided failure into 2 groups based on presence or absence of marginal bone loss on radiographs. Three typical implant outcomes in periapical film were shown in *Figure 2*. They were classified and labeled based on consensus by two experienced implant surgeon CNZ and YXG (certified specialist in implant dentistry with more than 7 years' experience). Detailed information of patients and implants were presented in *Table 1*.

Indications for panoramic imaging included suspicion of erratic extraction socket healing, postoperative implant position check, re-imaging prior to re-implant surgery, and review of multiple implants across different timepoints. Indications for periapical films included checking crown position, dental review across different timepoints, evaluation of bone structure, preoperative information gathering, and checking of the implant axis postoperatively. We collected all radiographic information before implant outcome for model training. Thus, a total of 529 periapical radiographs and 551 panoramic radiographs were included in our dataset.
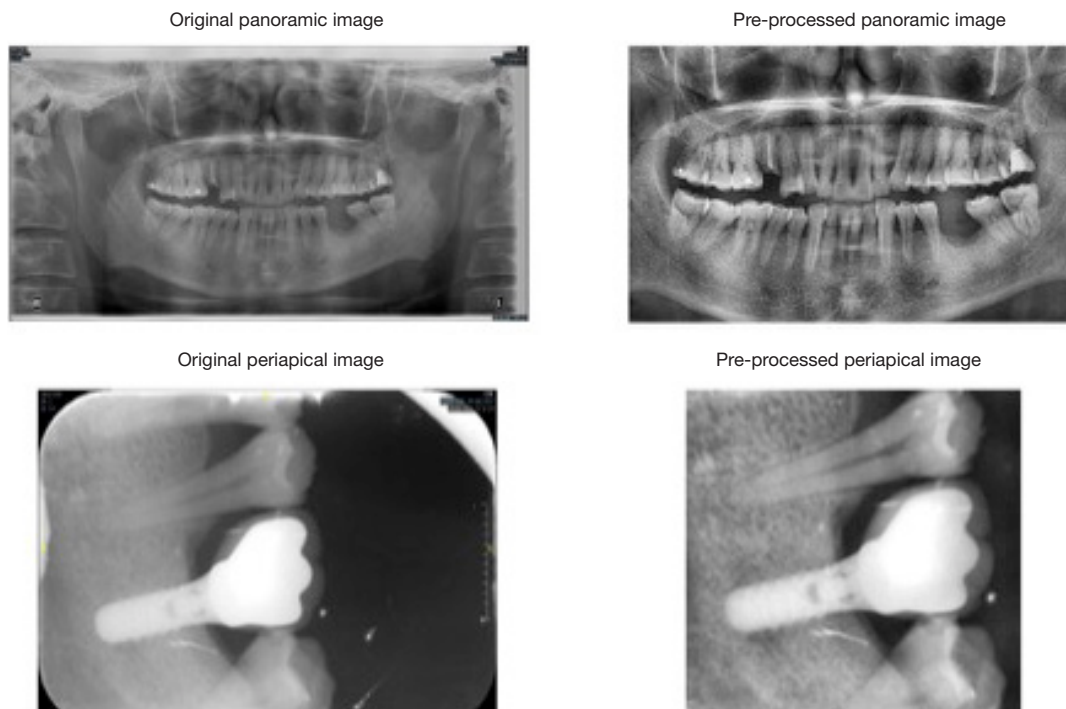
Original panoramic image

Pre-processed panoramic image

Original periapical image

Pre-processed periapical image

Figure 3 Cropped and histogram equalized panoramic and periapical images (implant with success). Pre-processed: cropping and histogram equalization were performed on periapical and panoramic radiographs to adjust the image contrast.

Training data and testing data

All pictures were saved as JPG format after downloading from PACS. A total of 529 periapical radiographs and 551 panoramic radiographs were included in our dataset. Periapical radiographs were cropped to show the implant and its vicinity. Panoramic radiographs were also cropped to an optimal position to remove irrelevant pixels. Histogram equalization was performed on periapical and panoramic radiographs to adjust the image contrast (example dataset was shown in *Figure 3*). All radiographs were resized to 224×224 pixels to meet the input size requirements of the deep learning model. Due to the unequal distribution of classes in the dataset, we augmented the dataset by randomly flipping and rotating (within 30 degrees) so that each class had the same number of images after augmentation (*Figure 4*). The augmented dataset had 900 panoramic radiographs and 900 periapical radiographs, which means that within the augmented dataset, each class had 300 panoramic radiographs and 300 periapical radiographs.

For data splitting, we used five-fold cross-validation to split the dataset into training and testing sets. In each fold, we randomly selected 720 panoramic radiographs and 720 periapical radiographs for training and used the remaining 180 panoramic radiographs and 180 periapical radiographs for testing. Five validation experiments were performed, with each fold used as the validation set and the remaining four as the training set. Therefore, each data point was used once for testing and four times for training. The cross-validation results from deep learning models were combined to measure the overall performance.

Architecture of deep convolutional neutral network

A pre-trained ResNet-50 deep convolutional neural network (CNN) was used for pre-processing, and the pre-trained weights were initialized by pre-trained ImageNet weights (22). The ResNet-50 architecture, which demonstrated excellent performance in the 2014 ImageNet Large Scale Visual Recognition Challenge, has preliminarily learned approximately 1.28 million images consisting of 1,000 object categories. It consists of 50 deep layers, and it is possible to obtain different scale features by applying convolutional filters of different sizes in the same layer. The training dataset was randomly separated into 32 batches for every epoch, and 1,000 epochs were run at a learning
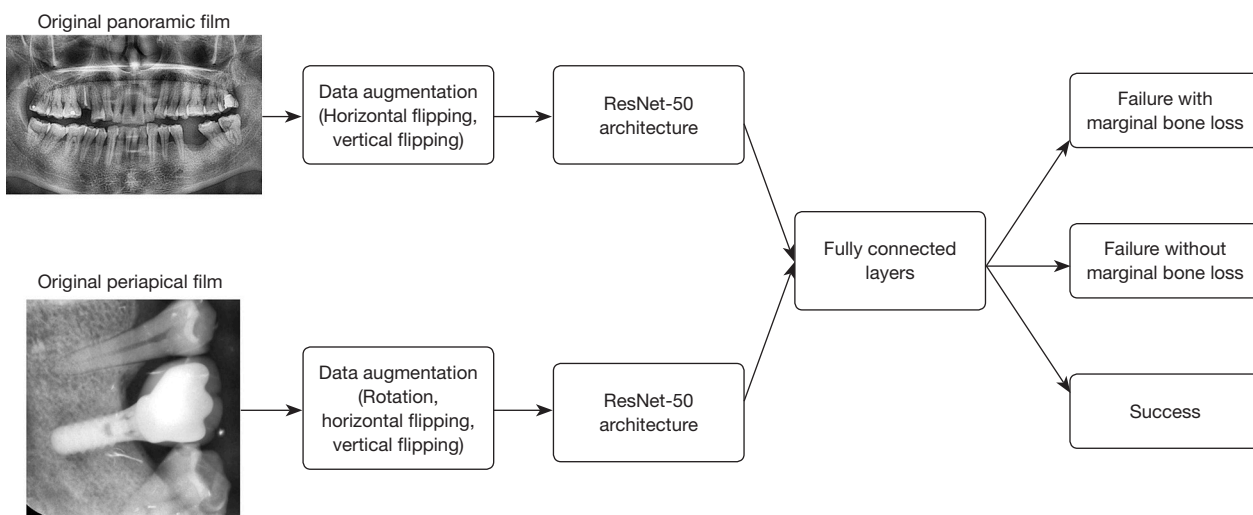
940

Zhang et al. Dental implant failure prediction from radiographic films

Figure 4 Architecture of the deep convolutional neural network model. ResNet-50 architecture: a pretrained deep CNN with 50 deep layers. CNN, convolutional neural network.

rate optimized by the Adam optimizer. To provide a better prediction of implant outcome, fine-tuning was used to optimize the weights and improve the output power by adjusting the hyperparameters.

Statistical analysis

A 5-fold cross-validation was used to estimate and create the optimal deep CNN algorithm weight factors. All deep CNNs in this study were implemented using Keras with TensorFlow in Python (Python Software Foundation, Fredericksburg, VA, USA). Data was split into training and testing datasets (4:1) using a 5-fold cross-validation. Periapical and panoramic films are compared with pre-processed films in predicting implant failure. Comparison among three implant outcomes of ROC (receiver operating characteristic) curves was performed. The diagnostic accuracy, precision, recall, and F1-score of the test dataset were assessed. The formulae are as follows:

$$Accuracy = \frac{TP + TN}{TP + FP + FN + TN} \quad [1]$$

$$Precision = \frac{TP}{TP + FP} \quad [2]$$

$$Recall = \frac{TP}{TP + FN} \quad [3]$$

$$F1\ score = \frac{2 \times Recall \times Precision}{Recall + Precision} \quad [4]$$

Results

The dataset consisted of a total of 529 periapical images in three categories: (I) failure with marginal bone loss had 91 images; (II) failure without marginal bone loss had 155 images; and (III) success (283 images). The dataset also included a total of 551 panoramic images of the same three categories: failure with marginal bone loss had 87 images, failure without marginal bone loss had 171 images, and success (293 images). The number of pre and post-operative images for each subgroup were detailed in *Table 2*.

Figure 5 shows pre-processed periapical and panoramic films achieved better accuracy in predicting implant outcome.

A comparison in ROC curves of the deep CNNs for classification is shown in *Figure 6*. The model achieved an AUC (area under the ROC curve) of 0.972 for failure with marginal bone loss, 0.947 for failure without marginal bone loss, and 0.975 for success.

In all conditions, for periapical images alone, the diagnostic accuracy was 78.6%. The precision was 0.84, recall was 0.73, and F1-score was 0.75. For panoramic images alone, the diagnostic accuracy was 78.7%; the precision was 0.87, recall was 0.63, and F1-score was 0.66. Both periapical and panoramic images were used in hybrid model, and the prediction accuracy was 87.0%. The precision was 0.85, recall was 0.88, and F1-score was 0.85 (*Table 3*).

Table 2 The number of pre and post-operatory images for each subgroup

| Film type	Failure with marginal bone loss	Failure without marginal bone loss	Success	Sum
Periapical film	91	155	283	529
	Pre-operative 2; post-operative 89	Pre-operative 8; post-operative147	Pre-operative 5; post-operative 278	Pre-operative 15; post-operative 514
Panoramic film	87	171	293	551
	Pre-operative 46; post-operative 41	Pre-operative 83; post-operative 88	Pre-operative 156; post-operative 137	Pre-operative 285; post-operative 266
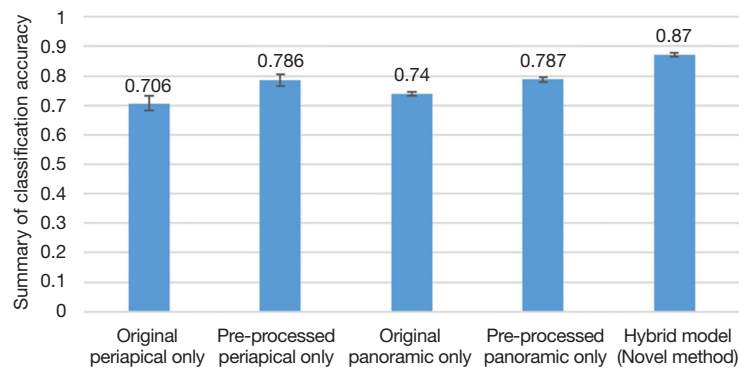
Figure 5 Classification accuracy of hybrid model compared to other four methods. Hybrid model: both periapical and panoramic images were used.
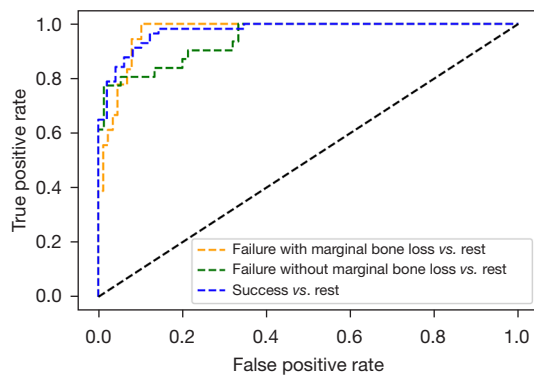
Figure 6 Multiclass ROC curve comparison for classification in implant outcomes. ROC, receiver operating characteristic.

Discussion

In this study, we developed a deep learning-based method to predict implant outcome using panoramic and periapical images. To the best of our knowledge, our study is the first implant outcome prediction model that used both periapical and panoramic images based on deep learning, achieving a prediction accuracy of 87.0%.

Panoramic and periapical images are the two most frequently analyzed image types in dental image analysis. Compared to CBCT, which is widely used in preoperative examination providing 3-dimensional view (23), panoramic and periapical imaging are generally more acceptable

Table 3 Evaluation for the prediction in implant outcome using periapical images, panoramic images, and hybrid images

Film type	Accuracy	Precision	Recall	F1-score
Periapical only	0.786	0.84	0.73	0.75
Panoramic only	0.787	0.87	0.63	0.66
Hybrid model	0.870	0.85	0.88	0.85

to patients and result in less radiation exposure. Similar to CBCT, panoramic images are often used in clinical examinations before implantation. For uncomplicated cases, panoramic view with careful clinical examination is enough. Periapical films are often used to assess postoperative implant osseointegration and the condition of the implant surroundings. However, CBCT is not recommended routinely after implantation. Therefore, osseointegration status, as assessed using periapical film, could instead be used to predict implant outcomes. Our study thus combined panoramic and periapical film to build a prediction model.

Alveolar bone structure assessment and tooth segmentation in panoramic film are most studied in literature (24-26). U-net or mask R-CNNs are often used as the backbone for different segmentation models for panoramic radiographs. In implant dentistry, panoramic images are often used to identify alveolar bone status and predict peri-implant marginal bone loss (27). Most studies have demonstrated a high accuracy and excellent reliability in automatic diagnosis (28-30).

Unlike panoramic images, periapical films provide detailed information focusing on root and surrounding bone areas containing three to four teeth. CNN has been built to classify dental diseases such as dental caries, periapical infection, periodontitis and prediction of periodontally compromised teeth (31,32). Due to its ability to record delicate structures, such as bone-to-implant contact, periapical films are often used to evaluate implant osseointegration, a key factor in implant survival, which would otherwise be assessed by clinicians subjectively. Deep learning based detection algorithm for images might be helpful for this task.

It is difficult to obtain both good coverage and peri-implant details from a single image type. A hybrid of both image types might mitigate this, as panoramic images show general features (for example, alveolar bone at the implant site compared to surrounding structures), while periapical images show specific details near the implant (for example, osseointegration status). Thus, hybrid model in our study achieved better prediction accuracy.

It is difficult to compare with other studies since research on the use of hybrid images for dental studies is limited. Some studies used a combination of bitewing and periapical images to detect teeth (33) or a set of periapical and panoramic images to detect dental disease and tooth structures (34). These methods focused on general dental analysis. None of them have attempted to find correlations between hybrid images and treatment outcome.

Moreover, previous work used traditional image processing techniques, such as thresholding with morphology, iterative thresholding, fuzzy clustering, and graph-based clustering, which inevitably neglect relevant information in the images. Our approach involves a deep learning-based implant failure prediction method using dental periapical and panoramic films. With a CNN and shared fully connected layers, the features from periapical and panoramic films are combined to help predict the occurrence of implant failure. Compared to traditional methods, such as thresholding methods, our CNN considers the spatial characteristics of an image and avoids information loss from thresholding.

The prediction accuracy in our study is high compared studies from other research fields (35,36). Aside from the hybrid technique, alveolar bone characteristics identified on radiographic film can also provide some indication of implant outcome (37,38). For example, a recent study revealed that relatively poor blood supply with thick cortical plates and small medullary spaces in dense bone of the mandible may be associated with implant failure (4). Moreover, a higher failure rate of posterior maxillary implants has also been noticed in clinic: the posterior region of the maxilla has loose bone trabeculae with a thin cortical layer; and insufficient residual bone heights in panoramic films are often observed (39). Meanwhile, implant osseointegration status in a periapical film could be ambiguous, if loaded before fully osseointegration, a higher risk of implant failure could be anticipated. In fact, most films in our study were pre-operative panoramic and post-operative periapical films, from which peri-implant alveolar bone characteristics might enrich the features for deep learning classification, however, it has to be validated by further interpretable deep learning research.

Based on clinical observation of radiographic alveolar bone pattern, two types of implant failure could be seen. The first type, often observed after loading, presents an obvious marginal peri-implant bone resorption. Many of these cases are associated with peri-implantitis. The second type, often seen before loading, presents a somewhat ambiguous radiolucent gap without obvious marginal peri-implant bone loss, whose histopathological mechanism is not clear. Thus, in our study, we divided implant failure outcome into two categories: implant failure with marginal bone loss and failure without marginal bone loss.

Using a model with 2 distinct types of failure outcome may provide more clinically useful data. For example, if a failure with marginal bone loss were predicted, an early

intervention, such as occlusal force adjusting, professional inflammation control or soft tissue grafting, should be performed accordingly. Moreover, if failure without marginal bone loss were predicted, this may be a sign of inadequate osseointegration around the implant, and a longer osseointegration period would be required. To better avoid implant failure, cautions should be paid when dense alveolar bone including constantly lifting while drilling with icy water irrigation during surgery with primary stability control under 45N. In the case of soft bone, erratic healing at the extraction site should be anticipated, and granulation tissue curettage may be required. Implant primary stability should be at least 5–10N.

The main limitation of the present study is its retrospective nature, especially the manual matching with gender, age and implant surgeon, which could have affected the analysis results. As we focus on alveolar bone characteristic in radiologic films, future matching variables should include bone quality, bone quantity and peri-implant osseointegration status before loading. Moreover, to increase learning performance and apply this system in clinical practice, a larger number of implant images and longer follow-up will be needed in the subsequent studies. Last but not the least, future study could combine CBCT images to have more comprehensive prediction model. Because of methodological discrepancies, comparisons among different studies were not feasible. Thus, results should be interpreted with caution.

Conclusions

The deep learning model learned features from periapical and panoramic images and predicted the occurrence of implant failure effectively. It might facilitate an early clinical intervention for potential implant failures.

Acknowledgments

Footnote

References

1. Guo J, Ban JH, Li G, Wang X, Feng XP, Tai BJ, Hu Y, Lin HC, Wang B, Si Y, Wang CX, Rong WS, Wang WJ, Zheng SG, Liu XN, Wang SC. Status of Tooth Loss and Denture Restoration in Chinese Adult Population: Findings from the 4th National Oral Health Survey. Chin J Dent Res 2018;21:249-57.
2. Gaêta-Araujo H, Oliveira-Santos N, Mancini AXM, Oliveira ML, Oliveira-Santos C. Retrospective assessment of dental implant-related perforations of relevant anatomical structures and inadequate spacing between implants/teeth using cone-beam computed tomography. Clin Oral Investig 2020;24:3281-8.
3. Jeong IC, Papapanou PN, Finkelstein J. Implant Failure Prediction Using Discriminant Analysis. Annu Int Conf

IEEE Eng Med Biol Soc 2019;2019:3433-7.

4. Camps-Font O, Martín-Fatás P, Clé-Ovejero A, Figueiredo R, Gay-Escoda C, Valmaseda-Castellón E. Postoperative infections after dental implant placement: Variables associated with increased risk of failure. J Periodontol 2018;89:1165-73.

5. Naseri R, Yaghini J, Feizi A. Levels of smoking and dental implants failure: A systematic review and meta-analysis. J Clin Periodontol 2020;47:518-28.

6. Chen J, Cai M, Yang J, Aldhohrah T, Wang Y. Immediate versus early or conventional loading dental implants with fixed prostheses: A systematic review and meta-analysis of randomized controlled clinical trials. J Prosthet Dent 2019;122:516-36.

7. Aghaloo T, Pi-Anfruns J, Moshaverinia A, Sim D, Grogan T, Hadaya D. The Effects of Systemic Diseases and Medications on Implant Osseointegration: A Systematic Review. Int J Oral Maxillofac Implants 2019;34:s35-49.

8. Annibali S, Pranno N, Cristalli MP, La Monaca G, Polimeni A. Survival Analysis of Implant in Patients With Diabetes Mellitus: A Systematic Review. Implant Dent 2016;25:663-74.

9. Revilla-León M, Gómez-Polo M, Vyas S, Barmak BA, Gallucci GO, Att W, Krishnamurthy VR. Artificial intelligence applications in implant dentistry: A systematic review. J Prosthet Dent 2021. [Epub ahead of print]. doi: 10.1016/j.prosdent.2021.05.008.

10. Nicolielo LFP, Van Dessel J, Jacobs R, Quirino Silveira Soares M, Collaert B. Relationship between trabecular bone architecture and early dental implant failure in the posterior region of the mandible. Clin Oral Implants Res 2020;31:153-61.

11. Huang N, Liu P, Yan Y, Xu L, Huang Y, Fu G, Lan Y, Yang S, Song J, Li Y. Predicting the risk of dental implant loss using deep learning. J Clin Periodontol 2022;49:872-83.

12. Schwarz F, Derks J, Monje A, Wang HL. Peri-implantitis. J Periodontol 2018;89 Suppl 1:S267-90.

13. Fiorellini JP, Sourvanos D, Sarimento H, Karimbux N, Luan KW. Periodontal and Implant Radiology. Dent Clin North Am 2021;65:447-73.

14. Berglundh T, Gislason O, Lekholm U, Sennerby L, Lindhe J. Histopathological observations of human periimplantitis lesions. J Clin Periodontol 2004;31:341-7.

15. Neto JDP, Melo G, Marin C, Rivero ERC, Cruz ACC, Flores-Mir C, Corrêa M. Diagnostic performance of periapical and panoramic radiography and cone beam computed tomography for detection of circumferential gaps simulating osseointegration failure around dental

implants: A systematic review. Oral Surg Oral Med Oral Pathol Oral Radiol 2021;132:e208-22.

16. Zhang CN, Zhu Y, Fan LF, Zhang X, Jiang YH, Gu YX. Intra- and inter-observer agreements in detecting peri-implant bone defects between periapical radiography and cone beam computed tomography: A clinical study. J Dent Sci 2021;16:948-56.

17. Lang MS, Miyamoto T, Nunn ME. Validity of fractal analysis of implants in individuals with healthy and diseased peri-implant mucosa. Clin Oral Implants Res 2020;31:1039-46.

18. Hung K, Yeung AWK, Tanaka R, Bornstein MM. Current Applications, Opportunities, and Limitations of AI for 3D Imaging in Dental Research and Practice. Int J Environ Res Public Health 2020.

19. Lee JH, Han SS, Kim YH, Lee C, Kim I. Application of a fully deep convolutional neural network to the automation of tooth segmentation on panoramic radiographs. Oral Surg Oral Med Oral Pathol Oral Radiol 2020;129:635-42.

20. Muramatsu C, Morishita T, Takahashi R, Hayashi T, Nishiyama W, Ariji Y, Zhou X, Hara T, Katsumata A, Ariji E, Fujita H. Tooth detection and classification on panoramic radiographs for automatic dental chart filing: improved classification by multi-sized input data. Oral Radiol 2021;37:13-9.

21. Tuzoff DV, Tuzova LN, Bornstein MM, Krasnov AS, Kharchenko MA, Nikolenko SI, Sveshnikov MM, Bednenko GB. Tooth detection and numbering in panoramic radiographs using convolutional neural networks. Dentomaxillofac Radiol 2019;48:20180051.

22. Deng J, Dong W, Socher R, Li LJ, Li K, Fei-Fei L. ImageNet: A large-scale hierarchical image database. 2009 IEEE Conference on Computer Vision and Pattern Recognition, 2009:248-55.

23. Jacobs R, Salmon B, Codari M, Hassan B, Bornstein MM. Cone beam computed tomography in implant dentistry: recommendations for clinical use. BMC Oral Health 2018;18:88.

24. Nishitani Y, Nakayama R, Hayashi D, Hizukuri A, Murata K. Segmentation of teeth in panoramic dental X-ray images using U-Net with a loss function weighted on the tooth edge. Radiol Phys Technol 2021;14:64-9.

25. Wang C, Peng C, Hou Y, Chen M. Augmented Reality Research of Measuring X-Ray Dental Film Alveolar Bone Based on Computer Image Analysis System. J Healthc Eng 2021;2021:5571862.

26. Murata M, Ariji Y, Ohashi Y, Kawai T, Fukuda M, Funakoshi T, Kise Y, Nozawa M, Katsumata A, Fujita H,

Ariji E. Deep-learning classification using convolutional neural network for evaluation of maxillary sinusitis on panoramic radiography. Oral Radiol 2019;35:301-7.

27. Zhang H, Shan J, Zhang P, Chen X, Jiang H. Trabeculae microstructure parameters serve as effective predictors for marginal bone loss of dental implant in the mandible. Sci Rep 2020;10:18437.

28. Takahashi T, Nozaki K, Gonda T, Mameno T, Wada M, Ikebe K. Identification of dental implants using deep learning-pilot study. Int J Implant Dent 2020;6:53.

29. Wang Y, Zhou L, Wang M, Shao C, Shi L, Yang S, Zhang Z, Feng M, Shan F, Liu L. Combination of generative adversarial network and convolutional neural network for automatic subcentimeter pulmonary adenocarcinoma classification. Quant Imaging Med Surg 2020;10:1249-64.

30. Zhu J, Zhang S, Yu R, Liu Z, Gao H, Yue B, Liu X, Zheng X, Gao M, Wei X. An efficient deep convolutional neural network model for visual localization and automatic diagnosis of thyroid nodules on ultrasound images. Quant Imaging Med Surg 2021;11:1368-80.

31. Lee JH, Kim DH, Jeong SN, Choi SH. Detection and diagnosis of dental caries using a deep learning-based convolutional neural network algorithm. J Dent 2018;77:106-11.

32. Lee JH, Kim DH, Jeong SN, Choi SH. Diagnosis and prediction of periodontally compromised teeth using a deep learning-based convolutional neural network algorithm. J Periodontal Implant Sci 2018;48:114-23.

33. Said EH, Nassar DEM, Fahmy G, Ammar HH. Teeth segmentation in digitized dental X-ray films using mathematical morphology. IEEE T on Inf Foren and Sec 2006;1:178-89.

34. Son LH, Tuan TM. Dental segmentation from X-ray images using semi-supervised fuzzy clustering with spatial constraints. Eng Appl of Artif Intel 2017;59:186-95.

35. Sun Y, Li C, Jin L, Gao P, Zhao W, Ma W, Tan M, Wu W, Duan S, Shan Y, Li M. Radiomics for lung adenocarcinoma manifesting as pure ground-glass nodules: invasive prediction. Eur Radiol 2020;30:3650-9.

36. Leung K, Zhang B, Tan J, Shen Y, Geras KJ, Babb JS, Cho K, Chang G, Deniz CM. Prediction of Total Knee Replacement and Diagnosis of Osteoarthritis by Using Deep Learning on Knee Radiographs: Data from the Osteoarthritis Initiative. Radiology 2020;296:584-93.

37. Sher J, Kirkham-Ali K, Luo JD, Miller C, Sharma D. Dental Implant Placement in Patients With a History of Medications Related to Osteonecrosis of the Jaws: A Systematic Review. J Oral Implantol 2021;47:249-68.

38. Do TA, Le HS, Shen YW, Huang HL, Fuh LJ. Risk Factors related to Late Failure of Dental Implant-A Systematic Review of Recent Studies. Int J Environ Res Public Health 2020.

39. Wu X, Chen S, Ji W, Shi B. The risk factors of early implant failure: A retrospective study of 6113 implants. Clin Implant Dent Relat Res 2021;23:280-8.